Supplement

Figure S1 shows fluorescence recovery curves for both fluorescein (hydrodynamic radius, R_H ~0.9nm and 50nm carboxylated polystyrene nanoparticles) acquired from FRAP experiments of oxCNFs. Experiments have shown that fluorescein exhibits no detectable binding interaction with oxCNFs and thus served here as a negative binding control. The curves have been normalized to the concentration of fluorescent species present in the ROI prior to photobleaching as intensity(t<0s)=1 and intensity(t=0s)=0 just after photobleaching. The oxide–coating applied to the CNFs was thin (the total oxCNF diameter after application of the coating was ~ 600 nm). *A thin oxide coating acts to minimize the oxCNF crowding effect on FRAP experiments by facilitating nearly unimpeded diffusion back into the ROI following photobleaching – diffusion is rapid*. In addition, a second and unintended factor also facilitated rapid diffusion into the ROI.

The PDMS sealing lids were found to periodically delaminate during the FRAP experiments where experiments were conducted on large oxCNF forests. Delamination occurred prior to both of the recovery experiments shown in figure S1. The effect of the delamination event was to provide an obstacle free pathway for fluorescent and unbleached species to rapidly diffuse into the ROI following photobleaching. As a result, even though the fluorescein dye was dissolved in 75%V glycerol (D = 0.25 $\mu m^2\ s^{-1}$) to render the diffusion flux of this small molecule detectable by FRAP, diffusion into the ROI was rapid with the fluorescence reaching the pre–bleaching value after only ~90s (*in addition, the viscous glycerol solution was also used to render the diffusion coefficient of fluorescein comparable to that of the significantly larger, and thus slower diffusing, 50nm polystyrene nanoparticles*). However, the photobleached 50 nm bead solution *saturated* in intensity recovery at ~10% below the pre–

bleach intensity. This is a commonly observed phenomenon observed during FRAP experiments when binding events occur and is attributed to bound and bleached species remaining in the ROI with a mean stay time $\tau_{des} >> \tau_D$ characteristic diffusion time. It was also verified that the saturation was not caused by a slower rate of diffusion as shown in the inset to figure S1.

The inset (figure S1) shows fluorescence recovery curves, again for fluorescein and 50nm nanoparticles, wetting oxCNFs, where the photobleached fraction was equal for both species. In addition, the PDMS lids did not delaminate during these experiments. *It is important to note that the initial fluorescence recovery rates for both species is both rapid roughly the same*. Thus, the diffusion rate of unbleached molecules/nanoparticles into the ROI was roughly equal. However, the rate of fluorescence recovery deviates between the two cases at longer recovery times (the blue line fit to the 50nm data is intended to clarify the deviation between the two recovery curves). The 50nm nanoparticle solution exhibits a slower recovery at longer times due to the bound and bleached nanoparticle population on the oxCNF surfaces which occupies a significant fraction of the available volume in the ROI. Assuming that the fluorescence recovery at long times is rate–limited by the desorption of these CNF–bound nanoparticles, k_{des} was estimated to be 0.045 ± 0.010 s^{-1} where the fluorescence recovery was fit using the expression [43-44]

$$I_{recovery}(t) = 1 - C_1 exp(-k_{des}t)$$

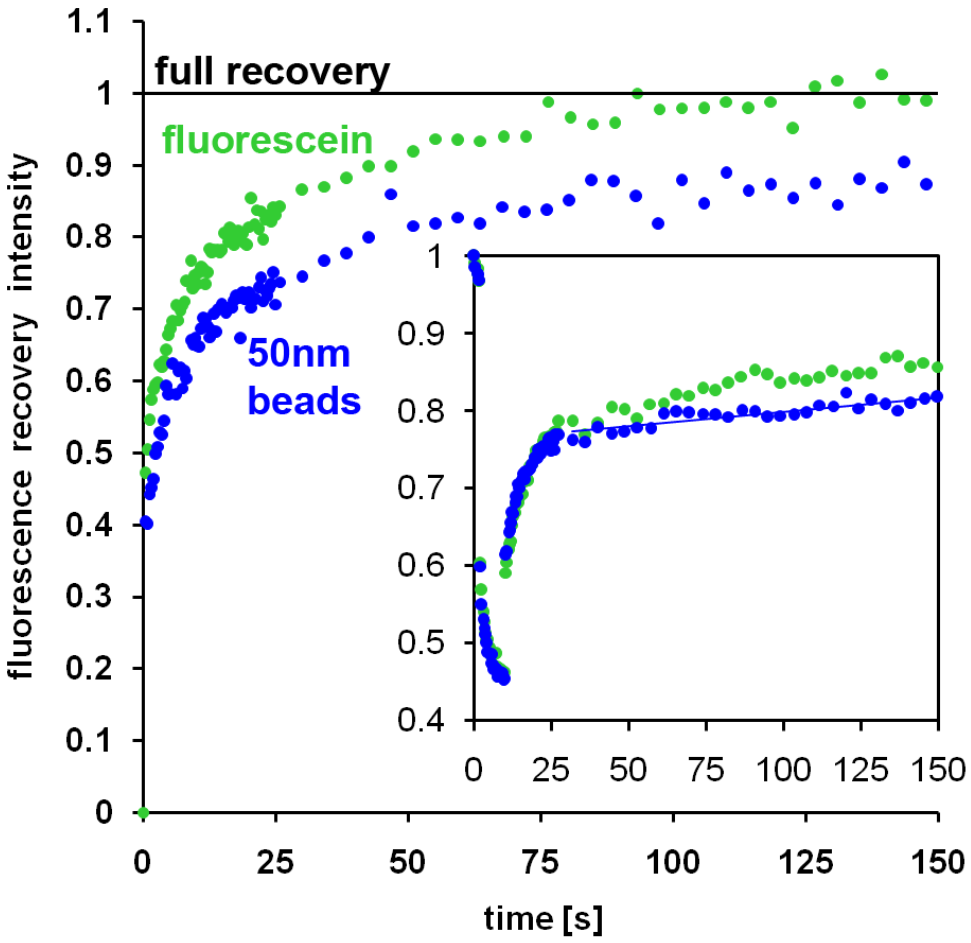

Figure S1 Fluorescence recovery after photobleaching (FRAP) curves for *green*) fluorescein dissolved in 75%glycerol (D_o=0.25 μm^2 s^{-1}) and *blue*) 50nm Fluoresbrite polystyrene carboxylated nanoparticles. Normalized to intensity(t<0s)=1 and intensity(t=0s)=0 regardless of the magnitude of photobleaching. For the inset, the normalization was the same except the intensity(t=0s) = true magnitude of photobleaching.